FULL-LENGTH PAPER

Genetic code expansion to enable site-specific bioorthogonal labeling of functional G protein-coupled receptors in live cells

Jordan M. Mattheisen[1,2] | Jaina S. Wollowitz[1,2] | Thomas Huber[1] | Thomas P. Sakmar[1]

[1]Laboratory of Chemical Biology and Signal Transduction, The Rockefeller University, New York, New York, USA

[2]Tri-Institutional PhD Program in Chemical Biology, New York, New York, USA

Correspondence
Thomas P. Sakmar, Laboratory of Chemical Biology and Signal Transduction, The Rockefeller University, 1230 York Ave, New York, NY 10065, USA.
Email: sakmar@rockefeller.edu

Abstract

For use in site-specific bioorthogonal labeling of expressed G protein-coupled receptors (GPCRs) in live cells, we developed a luciferase-based reporter assay. The assay was used to compare amber codon suppression efficiency, receptor functionality, and efficiency of different bioorthogonal labeling chemistries. We used the assay system to compare side-by-side the efficiency of incorporation of three different noncanonical amino acids [4-azido-L-phenylalanine (azF), cyclopropene-L-lysine (CpK), and *trans*-cyclooct-2-en-L-lysine (TCOK)] at three different sites on a GPCR using three different genetic code expansion plasmid systems. As a model GPCR, we engineered an epitope-tagged C-C chemokine receptor 5 (CCR5)-RLuc3 fusion for expression in HEK293T cells. Satisfactory incorporation of azF, CpK, and TCOK into heterologously expressed CCR5 was achieved. We also carried out cell-based calcium mobilization assays to measure the function of the engineered CCR5, and in the same cells, we performed bioorthogonal labeling of the engineered mutants using hetero-bivalent compounds containing bioorthogonal tethering groups linked to either a small-molecule fluorophore or a peptide. Favorable reaction kinetics of tetrazine-containing compounds with CCR5 harboring TCOK was observed. However, bioorthogonal labeling in live cells of CCR5 harboring CpK with tetrazine-containing compounds using the inverse electron demand Diels-Alder ligation was overall slightly more efficient than other reactions tested.

KEYWORDS
amber codon, bioorthogonal chemistry, genetic code expansion, GPCR, membrane protein, noncanonical amino acid

1 | INTRODUCTION

G protein-coupled receptors (GPCRs) are highly dynamic heptahelical membrane proteins that transduce diverse chemical stimuli into downstream cellular signaling cascades that mediate physiological responses. Genes for approximately 800 GPCRs are present in the human genome and understanding the molecular pharmacology

of GPCR signaling and regulation is an important area of systems biology research. GPCRs are targets for a large fraction of both FDA-approved and illicit drug entities. Developing novel strategies to advance orthosteric and allosteric ligands to modulate GPCR signaling is an essential area of pharmaceutical research.

A pivotal technology for studying GPCR structure and function is genetic code expansion (GCE), which allows for site-specific introduction of diverse noncanonical amino acids (ncAAs) at nonsense codons (often the amber, UAG codon) engineered into GPCRs. Pioneered by P. G. Schultz, GCE was applied to incorporate ncAAs translationally into proteins expressed in *Escherichia coli* (Wang et al., 2000, 2001; Wang & Schultz, 2001) and later in eukaryotic cells (Chin, Cropp, Anderson, et al., 2003; Chin, Cropp, Chu, et al., 2003). The first example of GCE applied to a GPCR was in the Ste2 receptor in yeast (Huang et al., 2008), but the methodology was also expanded to GPCRs expressed in mammalian cells (Ye et al., 2008, 2009, 2010). The general strategy involves transfecting mammalian cells in the presence an ncAA, with (1) a receptor plasmid engineered to contain a nonsense codon, along with (2) an aminoacyl-tRNA synthetase (aaRS) that acylates (3) an orthogonal aminoacyl-tRNA (aaT) with an anticodon recognizing the nonsense codon allowing it to be transported to the ribosome during protein translation. Successful suppression of a nonsense codon engineered into a GPCR gene allows incorporation of the ncAA and expression of a full-length mutant GPCR (Ye et al., 2008).

One significant advantage using GCE over other protein tagging techniques is that it allows for truly site-specific incorporation of an ncAA with unique functionality that minimally perturbs GPCR structure and function. For that reason, GCE has been the method of choice for studying GPCRs and has been used to install ncAAs with unique spectroscopic signatures (Wang et al., 2021; Ye et al., 2009, 2010), or photo-labile groups to facilitate targeted photo-crosslinking to map protein-protein (Gagnon et al., 2019; Grunbeck et al., 2012; Shah et al., 2020) or protein-ligand (Koole et al., 2017; Rannversson et al., 2016) interactions. In addition, introduction of ncAAs capable of undergoing bioorthogonal reactions can be used to tether fluorophores for direct imaging (Serfling et al., 2018, 2019) or to engineer fluorescence resonance energy transfer (FRET)-based or bioluminescence resonance energy transfer (BRET)-based biosensors to study GPCR dynamics (Kowalski-Jahn et al., 2021; Tian et al., 2022).

The efficiency of GCE in mammalian cells is still limited, which necessitates optimization of existing GCE systems to advance applications for studying challenging low-abundance membrane-protein targets such as GPCRs (Schmied et al., 2014). Reporter vectors containing green fluorescent protein (GFP) engineered to contain a nonsense codon or protein-GFP fusions have been used to monitor nonsense codon suppression (Serfling et al., 2018, 2019; Zhou et al., 2020), but suffer from low-sensitivity, nonlinear GFP fluorescence, and significant background due to autofluorescence in mammalian cell culture (Tsien, 1998). Bioluminescent protein reporters do not suffer from these drawbacks (Fan & Wood, 2007; Hall et al., 2012) and have been used to assess amber codon suppression efficiency, optimize cell transfection, and confirm orthogonality and specificity of amber suppressor aaRS/tRNA pairs in mammalian cells (Ye et al., 2008). A dual-luciferase-based reporter containing a Renilla luciferase (*Renilla reniformis*, RLuc) and firefly luciferase (*Photinus pyralis*, FLuc) fusion has also been used to monitor the successful concomitant incorporation of two ncAAs in mammalian cells (Kohrer et al., 2003). However, nonsense codon suppression efficiency can be dependent on codon context and the location of incorporation in the protein of interest (Wangen & Green, 2020). Direct side-by-side comparisons of multiple GCE systems and bioorthogonal labeling reactions for expressed GPCRs have not been reported.

Here we report a cell-based assay system to evaluate amber codon suppression efficiency, receptor functionality, and efficiency of different bioorthogonal labeling chemistries in expressed GPCRs. As a model GPCR, we engineered an epitope-tagged C-C chemokine receptor 5 (CCR5)-RLuc3 fusion for expression in HEK293T cells. We used the assay system to compare and contrast side-by-side the efficiency of incorporation of three different ncAAs (4-azido-L-phenylalanine (azF), cyclopropene-L-lysine (CpK), and *trans*-cyclooct-2-en-L-lysine (TCOK)) at three different sites on CCR5 using three different GCE plasmid systems. We also carried out cell-based calcium mobilization assays to measure the function of the engineered receptors. Finally, in the same cells, we performed bioorthogonal labeling of the engineered CCR5 mutants using heterobivalent compounds containing bioorthogonal tethering groups linked to a small-molecule fluorophore or a peptide. We report satisfactory incorporation of azF, CpK, and TCOK into heterologously-expressed CCR5. Bioorthogonal labeling of CCR5 in live cells between CpK and tetrazine-containing compounds using the inverse electron demand Diels-Alder (IEDDA) ligation was overall slightly more efficient than other reactions tested.

2 | RESULTS

2.1 | Design of aminoacyl tRNA synthetase-tRNA pairs

We compared experimentally three plasmid systems designed to facilitate ncAA incorporation through amber

codon suppression in mammalian cells. We focused on human C-C chemokine receptor 5 (CCR5), a well-studied GPCR, which mediates targeted cell migration and also serves as a co-receptor for human immunodeficiency virus-1 (HIV-1). We used HEK293T cells for the study because they are commonly used for heterologous expression and pharmacological studies of GPCRs. CCR5 was engineered to include RLuc (RLuc3), a modified luciferase enzyme, and a peptide epitope tag for the 1D4 monoclonal antibody (mAb) at the C-terminal tail (Figure 1a). The expression of full-length CCR5-RLuc3-1D4 can be

detected in cells using either a luminescence readout or reactivity with 1D4 mAb. Mutations in the CCR5-RLuc3-1D4 gene were introduced at three sites separately such that codons encoding amino acid residues F182, Y184, or L352 were replaced with amber stop codons (amb) using site-directed mutagenesis. F182 and Y184 are situated in the extracellular loop 2, and L352 is situated in the C-terminal tail of CCR5 (Figures 1b and S1).

Co-transfection of a CCR5-RLuc3-1D4 amb mutant with plasmids encoding for necessary amber codon suppression machinery (an orthogonal aminoacyl tRNA synthetase (aaRS)/tRNA pair) in the presence of ncAA should result in the translation of full-length CCR5-RLuc3-1D4 harboring the ncAA. The overall efficiency of amber codon suppression can be assessed using a luciferase reporter assay as described below. The first system we evaluated utilizes the *E. coli* tyrosyl-tRNA synthetase (TyrRS) and *Bacillus stearothermophilus* suppressor tRNA (*TyrT*) (Chin, Cropp, Anderson, et al., 2003; Ye et al., 2009). This amber codon suppression pair is encoded on two separate plasmids for incorporating the ncAA azF (Figure 1c,d). The other two systems we evaluated are from the pyrrolysl-tRNA synthetase (PylRS) and suppressor tRNA (PylT) system. The CpK incorporation system is a single plasmid containing one copy of a CMV promoter-driven *Methanosarcina bakeri* PylRS and four copies of U6 promoter-driven PylT (Figure 1e; Schmied et al., 2014). The TCOK incorporation system includes a single plasmid with one copy of EF-1α promoter-driven *M. mazei* PylRS and four copies of 7SK promoter-driven PylT (Figure 1f) and another plasmid containing four additional copies of PylT (Figure 1g).
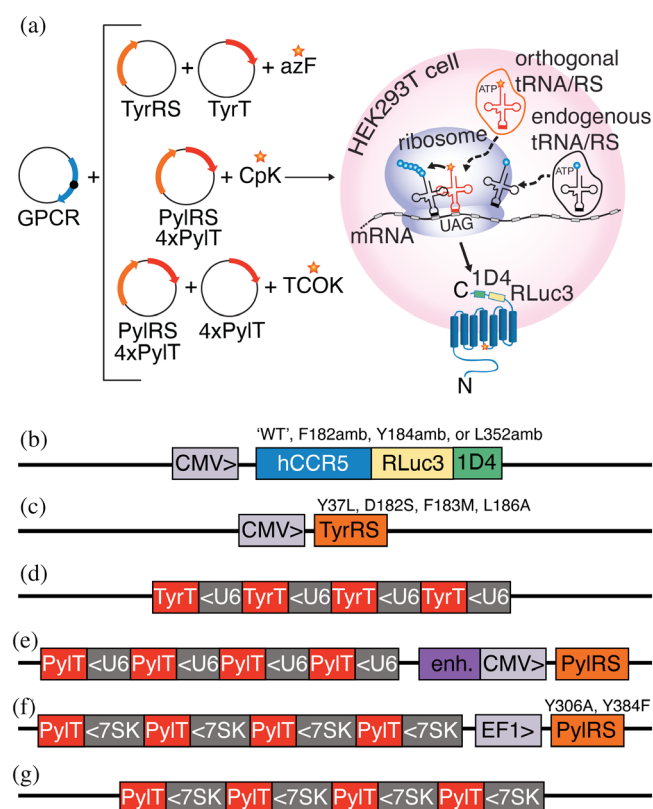

FIGURE 1 Incorporation of noncanonical amino acids in GPCRs expressed in mammalian cells. (a) HEK293T cells are transfected with plasmids containing an engineered GPCR amber mutant and orthogonal tRNA/synthetase pair and grown in the presence of noncanonical amino acid (4-azido-L-phenylalanine (azF), cyclopropene-L-lysine (CpK) or trans-cyclooct-2-en-L-lysine (TCOK)) to yield a full-length mutant GPCR-Renilla luciferase (RLuc3)-1D4 fusion. Plasmid maps are shown in B through G. (b) CCR5-RLuc3-1D4 fusion. (c) Tyrosyl-tRNA synthetase (TyrRS) for azF incorporation. (d) Multicopy tyrosyl-tRNA (TyrT) for azF incorporation. (e) Multicopy pyrrolysyl-tRNA synthetase (PylRS) and tRNA (PylT) on a single plasmid for CpK incorporation. (f) Multicopy PylT and PylRS on a single plasmid for TCOK incorporation. (g) Multicopy PylT for TCOK incorporation. CMV > = cytomegalovirus promoter, enh.
CMV = cytomegalovirus major immediate early enhancer, EF1 > = EF-1α promoter

2.2 | Luciferase-based reporter assay to evaluate amber codon suppression efficiency

We developed a luciferase-based reporter assay where suppression of an amber codon in CCR5-RLuc3-1D4 can be quantitated by measuring luminescence upon addition of RLuc substrate to cells (Figure 2a). We began by evaluating the impact of increasing the amount of plasmid encoding aaRS on the amber codon suppression efficiency while maintaining constant amounts of CCR5-RLuc-1D4 and tRNA DNA. We also measured the suppression efficiency for amber codons at three different sites in CCR5-RLuc3-1D4 (F182amb, Y184amb, and L352amb).

For the TyrRS/TyrT^{azF} system, as the amount of TyrRS increased, the percent luminescence relative to CCR5 wt also increased (Figure 2b). The increase for the
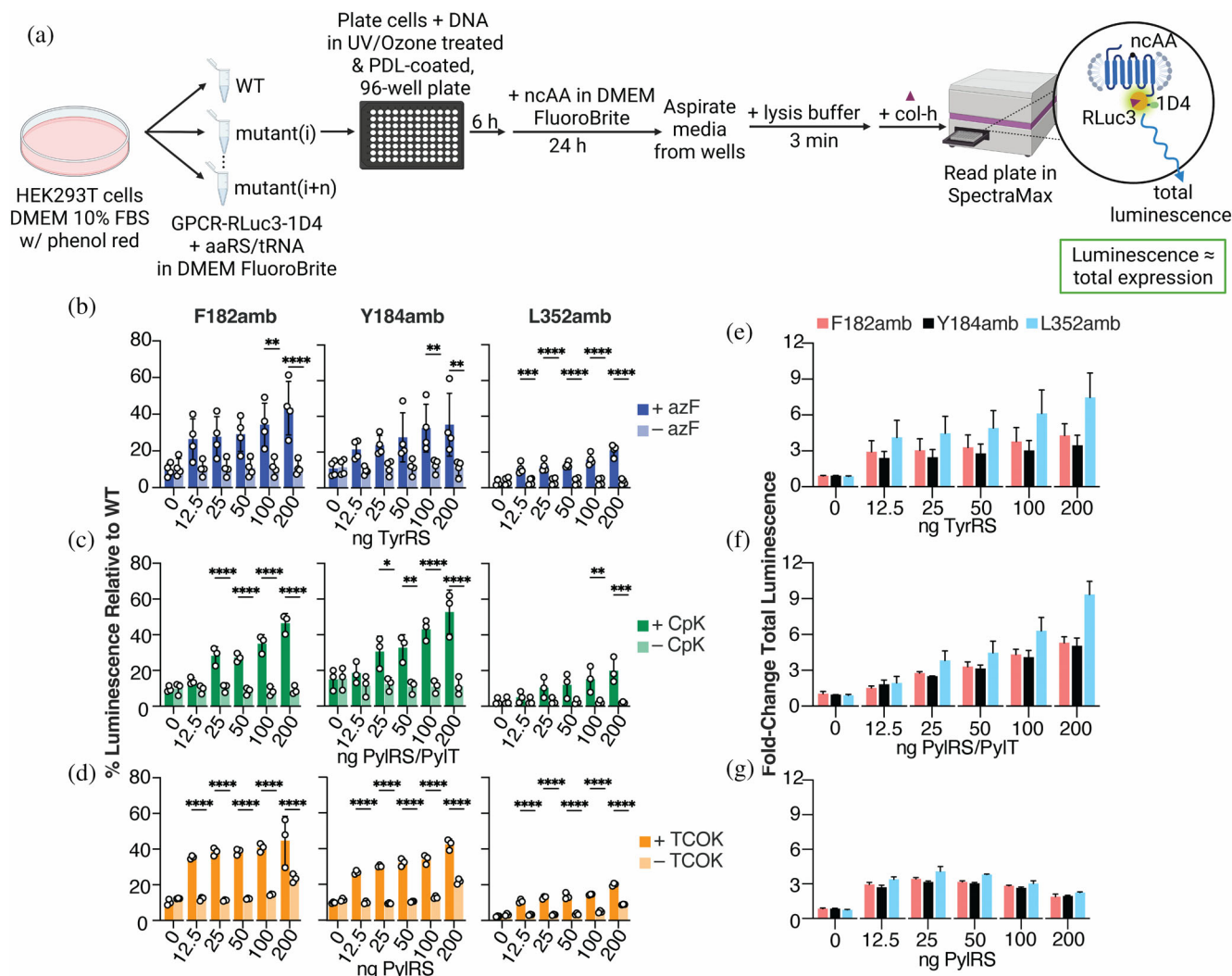
FIGURE 2 Luciferase assay system to evaluate efficiency of three amber codon suppression systems. (a) Workflow schematic. Total luminescence indicates expression level of full-length GPCR and is proportional to amber codon suppression efficiency. (b–d) Bar charts showing percent luminescence of cells transfected with CCR5-RLuc3-1D4-F182amb, -Y184amb, or -L352amb and varying amounts of aaRS plasmids. Luminescence was evaluated in the presence or absence of the ncAAs azF (blue), CpK (green), or TCOK (orange). Points are mean ± SD. (e–f) Bar chart showing fold-change of luminescence of CCR5-RLuc3-1D4-F182amb (light red), -Y184amb (black), or -L352amb (light blue) in the presence or absence of ncAA. Bars are mean ± SEM

F182amb and Y184amb mutants was 26%–40%, while the background signal as determined in the absence of ncAA was 11%. A similar trend was observed for PylRS/PylT^{CpK} machinery despite being titrated together on a single plasmid (Figure 2c). The F182amb and Y184amb suppression went from 12% to 50% while the background was again 11%. For PylRS/PylT^{TCOK} the amb suppression efficiency for F182amb and Y184amb ranged from 35% to 45% as the PylRS increased (Figure 2d). Interestingly, the background luminescence was 10% in all cases except at the highest amount of PylRS tested where the background jumped to more than 20%. For each of the GCE machinery systems tested, we observed that amber codon suppression efficiency was similar for the F182amb and Y184amb mutants. However, for the L352amb mutant

the overall suppression efficiency was consistently lower (only about 20%) with lower background signal (about 3%) as well. The relative fold-change in total luminescence was higher for the L352amb mutant than for the F182amb or Y184amb mutants for all three systems (Figure 2e–g).

2.3 | Functionality of CCR5 mutants harboring ncAAs

We next used a cell-based intracellular calcium mobilization assay to evaluate the ability of the expressed CCR5-RLuc3-1D4 constructs harboring ncAAs or empty vector (mock transfected plasmid) to get to the cell

surface and be activated by the agonist chemokine RANTES. CCR5 is not endogenously expressed in HEK293T cells, and RANTES is not able to cross the plasma membrane. Only corrected folded receptors at the cell surface should respond to RANTES and medicate intracellular calcium flux. Furthermore, the calcium mobilization assay was carried out in the same cells previously transfected with the CCR5-RLuc3-1D4 amb mutants and the amber codon suppression plasmids in the presence of the appropriate ncAA (Conklin et al., 1993; Lorenzen et al., 2018). Cells expressing CCR5-RLuc3-1D4 azF mutants and CCR5 wt demonstrated a similar dose-dependent increase in calcium mobilization upon stimulation with RANTES (Figure 3a). Furthermore, the agonist-induced calcium mobilization was inhibited by pretreatment of cells with the CCR5 antagonist drug maraviroc (mvc). A similar effect was seen for cells expressing CCR5-RLuc3-1D4 CpK mutants; however, the maximum relative calcium mobilization for F182CpK and Y184CpK mutants was about 80% of the

CCR5 wt response (Figure 3b). The CCR5-RLuc3-1D4 TCOK mutants F182TCOK and Y184TCOK also demonstrated 45% and 35%, respectively, lower degrees of calcium mobilization compared to CCR5 wt in response to RANTES. The calcium response curves relate to the overall efficiency of the amber suppression since only full-length receptors, which harbor the site-specific ncAA, are expected to be functional. In all cases the suppressed CCR5-RLuc3-1D4 L352amb mutants responded with a similar maximum calcium mobilization when compared with CCR5 wt. This result was expected since even receptors truncated at position 352 are expected to be functional as discussed below.

2.4 | Site-specific bioorthogonal labeling of CCR5 mutants using tetherable fluorophores and peptides

To demonstrate the ability to label functional CCR5 mutants harboring different ncAAs in live cells, we compared two bioorthogonal reaction chemistries. To label CCR5-azF mutants we chose dibenzocyclooctyne (DBCO) reagents, which undergo the bioorthogonal strain-promoted [3 + 2] azide-alkyne cycloaddition reaction (SPAAC) with azF (Figure 4a) (Agard et al., 2004; Dommerholt et al., 2010, 2016). For labeling CCR5-CpK mutants and CCR5-TCOK mutants, we used tetrazine (Tet)-containing reagents, which undergo inverse electron-demand Diels-Alder (IEDDA) reactions with CpK or TCOK (Figure 4b,c) (Blackman et al., 2008; Lang et al., 2012).

We separately coupled in live cells two different molecules to each mutant CCR5, a small molecule fluorophore or a peptide. For the fluorescent labeling of the CCR5 mutants we used either a DBCO-fluorophore (DBCO-680) or a Tet-conjugated fluorophore (Tet-680) (Figure 4e). Full-length CCR5-RLuc3-1D4 was detected using immunoblotting against the C-terminal 1D4 epitope tag and the labeled receptor was measured through direct fluorescent detection in the 700 nm channel. As expected, CCR5 wt was more highly expressed than the CCR5-amb mutants. The CCR5-CpK mutants and CCR5-TCOK mutants treated with Tet-680 showed similar labeling patterns. CCR5 wt samples were unlabeled, F182amb and Y184amb mutants were strongly labeled, and L352amb mutants were only moderately labeled. Y184amb was the most highly labeled CpK mutant and F182amb was the most highly labeled TCOK mutant.

Next, we performed posttranslational epitope tagging of CCR5-amb mutants expressed in live cells using DBCO-conjugated or Tet-conjugated OLLAS peptides (Figure 4f). The synthesis and characterization of DBCO-
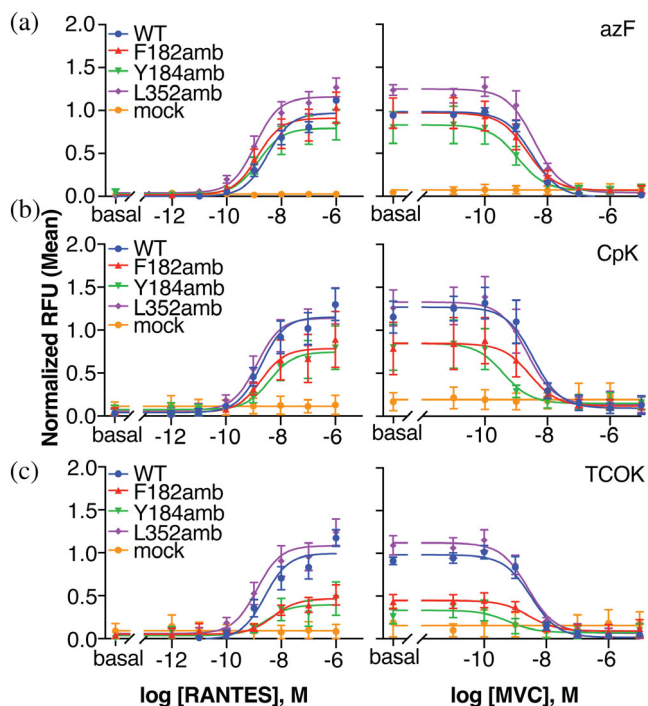

FIGURE 3 Functional characterization of CCR5 mutants engineered to contain ncAAs. Calcium mobilization of CCR5amb mutants or empty vector (mock) after genetic code expansion using three different ncAA incorporation systems. (a) azF-, (b) CpK-, and (c) TCOK-RS/tRNA pairs in the presence of appropriate ncAA. Left panel, dose–response of calcium mobilization stimulated by CCR5 agonist RANTES. Right panel, dose–response inhibition of RANTES-induced calcium mobilization (0.1 μM) after preincubation with CCR5 antagonist maraviroc (mvc). Points are mean fluorescence ± SEM normalized to CCR5-WTazF in $n = 3$–5 experiments
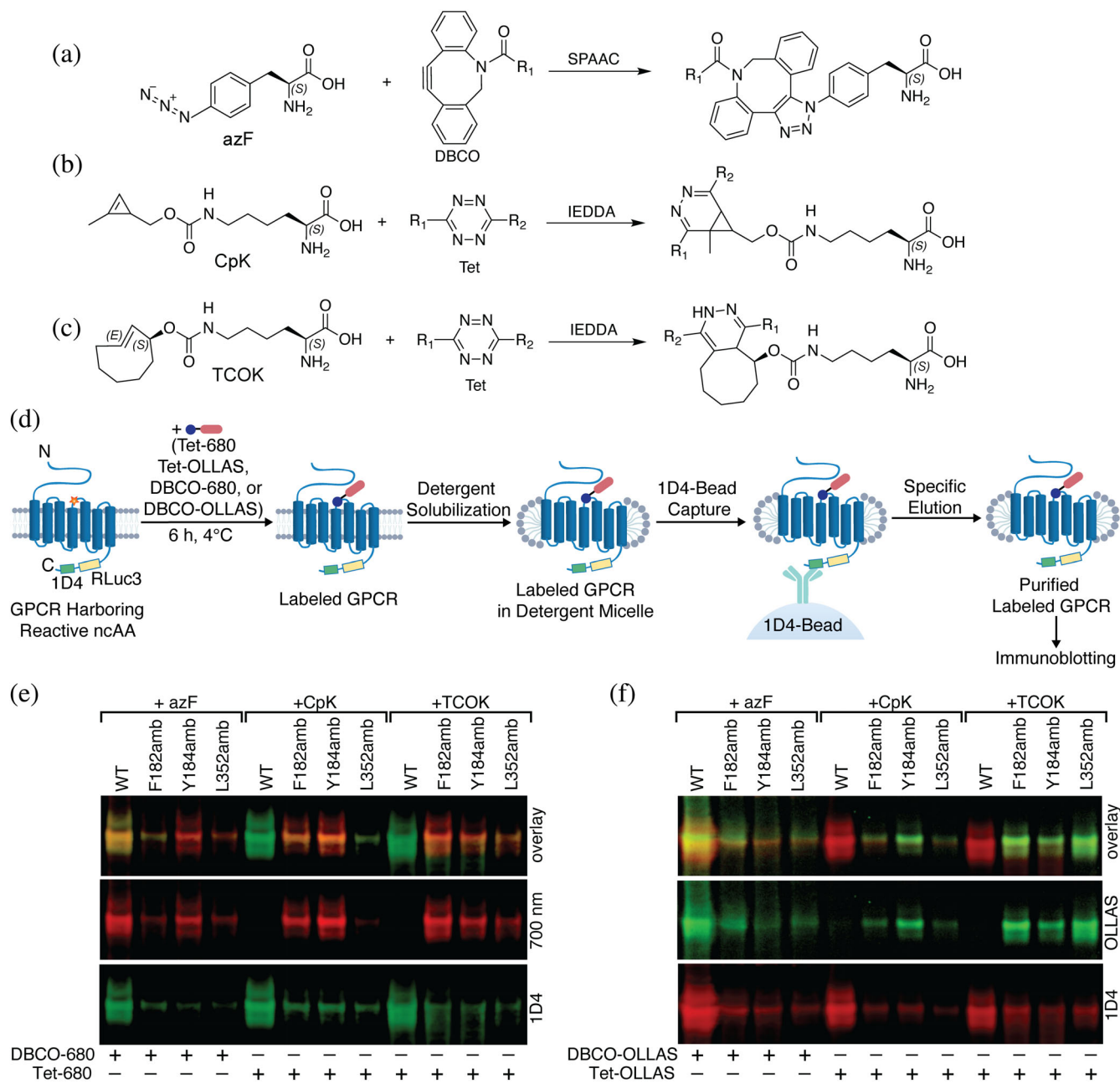
FIGURE 4 Live-cell bioorthogonal labeling of GPCRs engineered to contain ncAAs. (a) Strain-promoted azide-alkyne cycloaddition (SPAAC) between azF and DBCO-containing compounds. (b) Inverse electron-demand Diels-Alder ligation (IEDDA) between tetrazine-containing compounds and CpK or (c) TCOK. (d) Live-cell labeling workflow schematic. (e) Immunoblot showing total CCR5-RLuc3-1D4 expression (green) and receptor labeled by bioorthogonal fluorophore (DBCO-680 or Tet-680, red). (f) Immunoblot showing total mutant CCR5-RLuc3-1D4 expression (red) and receptor labeled by bioorthogonal peptides (DBCO- or Tet-OLLAS, green). *Source Data*: Figure e, f: raw immunoblots showing live cell bioorthogonal labeling of CCR5

OLLAS and Tet-OLLAS is described in the methods and Figure S3. The full-length receptor was detected using a mAb against the C-terminal 1D4 epitope tag and the bioorthogonal labeling was detected using a mAb against the OLLAS peptide. Cells expressing CCR5 wt and treated with Tet-OLLAS did not appear to be labeled. Of the CpK mutants, Y184CpK was the most highly labeled. For TCOK mutants, all were highly labeled, including L352amb which was not significantly labeled by the Tet-

680 fluorophore. Importantly, CCR5 wt was highly labeled using both DBCO-680 and DBCO-OLLAS indicating undesired and nonspecific background labeling.

3 | DISCUSSION

The first aim of this study was to compare experimentally three plasmid systems designed to facilitate site-specific

ncAA incorporation of azF, CPK, and TCOK into expressed GPCRs using amber codon suppression in mammalian cells. We focused the comparison on human C-C chemokine receptor 5 (CCR5), a well-studied GPCR, which mediates targeted cell migration, and also serves as a co-receptor for human immunodeficiency virus-1 (HIV-1). The second aim of the study was to compare two different bioorthogonal labeling chemistries carried out in live cells expressing the mutant GPCRs harboring the ncAAs. The chemistry was carried out in the same cells used for the amber codon suppression.

In order to compare different amber codon suppression systems with the aim of incorporating ncAAs into functional GPCRs, we developed a cell-based luciferase reporter assay system. Results from the luciferase assay indicated variability in amber codon suppression efficiency when using the TyrRS/TyrT^{azF} system. Since the TyrRS and TyrT are on separate plasmids and they must be co-transfected in the same cell for amber suppression to occur, the variability in efficiency is not totally unexpected. Using the PylRS/PylT systems, which both have single plasmids encoding the PylRS and copies of the PylT, we saw less variability and generally higher suppression efficiency. In general, it might be advantageous when possible to include all amber suppression components on a single plasmid, although more experiments would needed to understand the contributions of the different promoters and gene copy numbers to make firm conclusions.

We found that the L352amb mutants had lower amber suppression efficiency and background signal compared with amb mutations at the other sites tested. Since L352 is situated next to the stop codon of the CCR5 gene, we hypothesize that the codon context at this residue contributes to high fidelity translation termination (Wangen & Green, 2020). For the TCOK amber suppression machinery, we observed that the lowest amount of PylRS transfected plasmid resulted in the highest efficiency of amber suppression (nearly 40%) compared with the CpK and azF amber suppression machinery (20% and 25%, respectively). However, as the RS component was increased, the peak amber suppression remained approximately the same for the TCOK system, while it increased for the azF and CpK systems. We also observed a significant increase in background luminescence at the highest concentration of PylRS for TCOK incorporation, suggesting possible read-through suppression even in the absence of added TCOK. This background was not observed for the other two systems. However, the total amount of PylRS was not identical for the two systems, making a direct quantitative comparison difficult. The salient finding is that we observed the most efficient overall suppression relative to background using the CpK system as described.

Cell-based calcium mobilization assays were carried out in the same cell cultures used for amber codon suppression. Results from assays showed that azF, CpK, and TCOK substituted at three different positions in CCR5 did not significantly alter the ability of the agonist RANTES to activate the mutant receptors, nor the ability of the antagonist mvc to inhibit RANTES activation. Despite the overall lower efficiency of ncAA incorporation at L352amb, we observed that the L352amb mutants had the highest calcium mobilization responses. This result was expected because a truncation at L352 would result in a mutant CCR5 that is only one amino acid residue shorter than CCR5 wt.

We next carried out bioorthogonal surface labeling experiments. First, we evaluated labeling of CCR5-azF with the SPAAC reaction using either a DBCO-conjugated fluorophore and or DBCO-conjugated peptide, the epitope for OLLAS mAb. We found that treatment with either DBCO-680 or DBCO-OLLAS showed relatively high background labeling. This result was expected and was consistent with previously reported experiments that showed the ability of DBCO reagents to react nonspecifically with thiol groups (van Geel et al., 2012). We then evaluated labeling of CCR5-CpK and CCR5-TCOK mutants with the IEDDA reaction using Tet-conjugated fluorophores or Tet-conjugated OLLAS peptide. Satisfactory labeling was observed relative to background for both CpK and TCOK. Precise quantitation of immunoblotting data is difficult due to uncertainties about receptor enrichment during immunocapture as well the possibility of nonlinear mAb-epitope binding profiles. We envision future complementary flow cytometry experiments to achieve quantitative single-cell information regarding GCE labeling.

There were some differences between the extent of labeling when comparing the fluorophore and the peptide depending on the location of the ncAA, but these differences were not investigated further. However, they are most likely due to differences in local accessibility at the membrane-water interface between the fluorophore and peptide, and the presence of PEG linkers in the peptide conjugates. Despite the L352 residue being intracellular, we observed slight labeling of CCR5-L352CpK and CCR5-L352TCOK. We suspect that this was due to a small amount of cell lysis during the 6 h labeling reaction, or continued reaction that might have occurred between the time of cell lysis and gel electrophoresis of samples.

When evaluating different GCE systems for applications involving bioorthogonal labeling, overall amber codon suppression efficiency, total receptor expression, specificity and kinetics of the bioorthogonal reaction, and the stability of the ncAA and the bioorthogonal labeling reagent must be considered. For applications of GCE that

require bioorthogonal labeling of GPCRs, the overall yield of target labeling relative to background is paramount. Therefore, we compared the efficiency of labeling relative to background where target protein expression, amber suppression and bioorthogonal labeling were carried out in the same cells. However, we did employ the luciferase-reporter assay to compare and optimize the amber codon suppression systems. We then compared the labeling reactions using either direct fluorescence measurements in the case of the conjugated-680 or immunoblot analysis for the conjugated OLLAS peptide. We found that the IEDDA reaction was satisfactory to introduce site-specific labels in the GPCR model system at either CpK- or TCOK-containing CCR5 mutants. The methods and results described in this paper should prove useful for applications where site-specific fluorophore, or posttranslational peptide labeling of GPCRs in live cells is indicated (Huber & Sakmar, 2014; Naganathan et al., 2013; Tian et al., 2017).

4 | METHODS

4.1 | Plasmid construction

The plasmid CCR5-RLuc3-1D4 contains the human coding sequence of CCR5 (Ye et al., 2008), a mutant *Renilla Reniformis* Luciferase (Berchiche & Sakmar, 2016), and the C-terminal 1D4 epitope tag (DEASTTVSKTETSQVAPA) (Oprian et al., 1991) in a pcDNA3.1+ vector. The construct was assembled using NEBuilder HiFi DNA Assembly Kit (New England BioLabs, NEB) after amplification of CCR5 wt (from a plasmid containing CCR5-1D4) and the RLuc3-1D4 and plasmid backbone (from a plasmid containing CLTR2-RLuc3-1D4). Oligonucleotides for amplification steps were purchased at the standard desalting grade from Integrated DNA Technology. QuikChange lightning site-directed mutagenesis kit (agilent technologies) was used to engineer amber codon (UAG) mutations at positions F182, Y184, and L352 CCR5-RLuc3-1D4. Coding sequences were verified by sanger sequencing. For azF incorporation, one plasmid containing the *Bst*-Yam amber suppressor tRNA derived from *B. stearothermophilus* (tRNA^{Tyr}) and one plasmid containing the evolved *E. coli* TyrRS(Y37L/D182S/F182M/L186A) were used as described previously (Ye et al., 2008). For CpK incorporation, a single plasmid containing four copies of U6 promoter-driven suppressor tRNAs and one copy of a CMV promoter-driven *M. bakeri* PylRS provided by Simon Elsässer was used (Schmied et al., 2014). For TCOK incorporation, one plasmid containing PylRS and four copies of PylT and one plasmid containing four copies of PylT alone was used. The construct Gqi5 is a modified version of the

α subunit of Gq where the C-terminal amino acid residues are derived from the α subunit of Gi2 (such that EYNLV-COOH in Gq becomes DCGLF-COOH in Gqi5). Gqi5 is in the pcDNA3.1+ vector and is used to enable signaling of Gi-coupled receptors to Gq pathways as described previously (Conklin et al., 1993; Lorenzen et al., 2018).

4.2 | Cell culture

HEK293T cells (ATCC, CRL-11268), passage number 5–20, were maintained in Dulbecco's Modified Eagle Medium containing 4.5 g/L D-Glucose (DMEM-Gluta-Max, Gibco) and supplemented with 15 mM *N*-2-hydroxyethylpiperazine-*N'*-2-ethanesulphonic acid (HEPES, pH 7.5, Corning) and 10% (v/v) BenchMark fetal bovine serum (FBS, Gemini) or Fetal Bovine Serum Premium (FBS, Atlanta Biologicals, Inc.). Cells were maintained at 37°C and 5% CO_2.

4.3 | Amber codon suppression

The ncAA stocks for 4-azido-L-phenylalanine (azF) (Chem-Impex International, Inc.), N^6-[[(2-methyl-2-cyclopropene-1-yl) methoxy] carbonyl]-L-lysine (CpK), and *trans*-cyclooct-2-en-L-lysine (TCOK) (Sirius Fine Chemicals) were prepared to 100 mM in 0.2 M NaOH/15% dimethyl sulfoxide (DMSO) solution and stored in aliquots at −20°C until use. Aliquots were diluted 20-fold in 1 M HEPES prior to addition to cell culture medium. The final concentration of ncAAs in cell media was 0.5 mM.

4.4 | Luciferase assays

HEK293T cells were transfected and seeded into 96-well microtiter plate (polystyrene, black-walled, chimney, flat bottom, Greiner Bio-One) in a single operation. Briefly, 2.5 μl of Lipofectamine 2000 (Thermo Fisher Scientific) per μg DNA was diluted in FluoroBrite-DMEM (no FBS) and then added to an equal volume of DNA (225 or 250 ng per well) diluted in the same media. After 15 min, the mixture was combined with equal volume of cells in 2× FluoroBrite-DMEM (30 mM HEPES, 8 mM L-glutamine [Gibco], 20% FBS). Then 100 μl of this mixture containing approximately 21,000 cells was seeded into each well of a black-walled 96 well plates that were previously prepared by UV/ozone treatment for 8 min prior to 1 h incubation with 0.1 mg/mL poly-D-lysine (PDL, Sigma-Aldrich). The cells were incubated at 37°C and 5% CO_2. After 4–6 h, 100 μl of 1 mM ncAA in FluoroBrite-

DMEM (10% FBS, 15 mM HEPES, 4 mM L-glutamine) was added per well. The cells were returned to the incubator. Each well of the 96-well plate contained 25 ng receptor [wt, F182am, Y184am, L352am, or pcDNA (mock)] and 200 or 225 ng total of tRNA/RS DNA. For azF, the tRNA was held constant at 25 ng per well while the TyrRS was titrated from 0 to 200 ng per well. For CpK, the PylRS and tRNA are encoded on the same plasmid so both were simultaneously titrated from 0 to 200 ng per well. For both, the total DNA was kept constant at 250 ng/well by supplementing with pcDNA plasmid. For TCOK, the plasmid encoding the PylRS also encodes for four copies of the tRNA. To maintain the same amount of tRNA across all conditions, as the PylRS amount was increased, the amount of a secondary plasmid encoding four copies of the tRNA was titrated down by the same amount simultaneously with the total PylRS and tRNA plasmid DNA being kept constant at 200 ng per well. (i.e., 0 ng tRNA plasmid was transfected in conditions where 200 ng PylRS plasmid was used, 200 ng tRNA plasmid was transfected in conditions where 0 ng PylRS plasmid was used). Approximately 48 h after transfection, media was aspirated from the wells and replaced with 40 μl lysis buffer (25 mM Tris–HCl pH 7.8, 2 mM EDTA, 10% glycerol, 1% Triton×-100, 2 mM 1,4-dithiothreitol (DTT), 0.1% bovine serum albumin fraction V fatty acid-free (BSA)). The plate was shaken for 3 min at 400 rpm prior to the addition of 10 μl of 25 μM coelenterazine-h (col-h, NanoLight Technology) in lysis buffer to each well. Total luminescence was measured every 1 min 10 s for 10 min at 37°C using a SpectraMax i3x multi-mode microplate reader (Molecular Devices).

Each plate contained 9–12 wells which were transfected with pcDNA alone (min) or CCR5 wt alone (max) which were used to normalize the luminescence signal across each assay plate using the formula $sample_{NORM} = (sample-min)/(max-min)$. For each condition, three replicate wells were averaged and standard error was calculated (Figure S2). For each CCR5-amb mutant, the adjusted luminescence was calculated using the formula $sample_{ADJUSTED} = (sample_{NORM} - pcDNA_{NORM})/(wt_{NORM} - pcDNA_{NORM})$ separately for each concentration of RS in the presence or absence of ncAA. Finally, the fold-change was calculated by dividing the $sample_{ADJUSTED}$ by the $sample_{ADJUSTED}$ condition when no RS was present. The fold-change from three or four independent experiments were plotted in GraphPad Prism 9.4.0 with their standard deviation.

4.5 | Calcium mobilization

The day prior to transfection 700,000 HEK293T cells were seeded in 2 ml DMEM-complete media (15 mM HEPES, 4 mM L-glutamine, 10% FBS) into six-well plates. The following day cells were transfected with 3.5 μg total DNA using Lipofectamine 2000. The DNA ratios for azF CCR5:tRNA:TyrRS:Gqi5:pcDNA was 1:1:0.5:0.5:0.5, for CpK CCR5:tRNA/TyrRS:Gqi5 was 1:2:0.5, and for TCOK CCR5:tRNA:TyrRS/tRNA:Gqi5 was 1:1.75:0.25:0.5. Briefly, for each well DNA and 7 μl of Lipofectamine 2000 were diluted in 100 μl opti-MEM (Gibco) each. After 5 min, the lipofectamine mixture was added to the DNA and incubated at room temperature for 15 min prior to dropwise addition onto the plated cells. After 4–6 h, 1 ml media was removed from each well and replaced with DMEM-complete media containing ncAA for a final concentration of 0.5 mM. Plates were returned to 37°C and 5% CO_2 overnight. The following day media was aspirated from the wells, cells were washed with Dulbecco's phosphate-buffered saline (DPBS, Gibco) and trypsin–EDTA (0.25%, phenol red, Gibco) was used to dissociate cells from the plate. Cells were resuspended in DMEM-complete media supplemented with 0.5 mM ncAA and plated at a density of 21,000 cells per well in a prepared (UV/ozone-treated and PDL-coated) 384-well microtiter plate (polystyrene, black-walled, flat bottom, Greiner Bio-One). The cells were returned to the incubator overnight. Approximately 48 h after transfection calcium mobilization assay was performed. FLIPR Calcium six dye (Molecular Devices) was dissolved to 4× concentration in assay buffer HBSS-H (Hanks' Balanced Salt Solution [HBSS] with 20 mM HEPES, pH 7.4) with 0.4% (w/v) BSA. Then 10 μl of the dye was added to each well. Then 10 μl of assay buffer (for RANTES titration assays, Pepro-Tech, Inc.) or 10 μl of (4×) maraviroc prepared in assay buffer (for competition assays) was added and incubated with the dye for 2 h at 37°C, 5% CO_2. Maraviroc serial dilutions were prepared in DMSO prior to dilution in assay buffer and addition to cells (10 pM–10 μM final). After 2 h, the assay plate was transferred to a FlexStation II 384 plate reader (molecular devices) pre-warmed to 37°C, which injected 10 μl RANTES for final concentrations 1 pM–1 μM (for RANTES titration assays) or 0.1 μM (for competition assays). Fluorescence readings were collected with excitation at 485 nm, emission at 535 nm, and the dichroic mirror at 525 nm over a 100 s time course with 2.5 s intervals, with the stimulation ligand added to the cells with mixing 20 s after the start of measurement. Relative fluorescence units (RFU) were calculated as the mean signal between 20 and 100 s (raw injection signal) minus mean signal between 0 and 20 s (basal signal). The agonist and inhibitor dose curves for the wt_{azF} condition were plotted in GraphPad prism 9.4.0. The best-fit model was selected between a horizontal line versus a three-parameter fit for using Akaike's information criterion. Then all other conditions were normalized to the max and min values of the fit for the

agonist or inhibitor curves resulting in normalized RFU. Replicates from three to free experiments were plotted in GraphPad Prism and again fit to curves as described above.

4.6 | Live cell labeling

One day prior to transfection, 10 cm dishes were seeded with 4,000,000 HEK293T cells in 7 ml DMEM-complete media. The following day the cells were transfected in 3 ml opti-MEM with 17 μg total DNA using lipofectamine 2000 (2.5 μl/μg) according to manufacturer's instructions at the aforementioned DNA ratios used for Ca^{2+} mobilization assays. 4–6 h later, 250 μl of 20 mM stock ncAA in 1 M HEPES was added dropwise to the plates for 0.5 mM final concentration.

After 48 h, media was aspirated and each plate was washed with 3 ml warm DPBS. Then cells were scraped from the plate in 3 ml cold DPBS, transferred to 15 ml tubes, and pelleted at 500 RCF for 5 min at 4°C. The supernatant layer was aspirated off and the cell pellet was resuspended in 1000 μl labeling media (FluoroBrite-DMEM, 15 mM HEPES). Then 500 μl cell suspension was aliquoted into 1.7 ml tubes containing 500 μl of 100 μM DBCO-AzDye 680 or Tet-AZDye 680R (Click chemistry tools) or DBCO-OLLAS or Tet-OLLAS in labeling media. Peptides were synthesized by Proteomics Center at The Rockefeller University. A 25 μmol-scale Fmoc solid-phase peptide synthesis strategy was used. Peptides were synthesized using SYMPHONY multiple peptide synthesizer (Protein technologies). Peptides were purified to a purity between 79% and 91% using C18 based reversed phase chromatography and then conjugated to DBCO-PEG4-NHS ester or Tet-PEG5-NHS ester (Broad pharma). Cells were incubated while nutating at 4°C for 6 h. Cells were then pelleted at 500 RCF for 5 min, washed twice in 1 ml cold DPBS, then resuspended in 500 μl lysis buffer [50 mM Tris–HCl, pH 6.8, 100 mM NaCl, 1 mM $CaCl_2$, 1% n-dodecyl-β-D-maltopyranoside (DDM, Anatrace), 0.1 mM phenylmethylsulfonyl fluoride (PMSF, Sigma-Aldrich), 0.12 mg (0.552 units) aprotinin (Sigma-Aldrich), cOmplete Mini, EDTA-free protease inhibitor cocktail (Roche)] and mutated for 1 h, 4°C. Samples were centrifuged for 30 min at 21,000 RCF, 4°C.

1D4-sepharose resin was prepared as described earlier (Knepp et al., 2011; MacKenzie et al., 1984). Approximately 1250 μl resin slurry (625 μl packed resin) was washed three times in 2 ml DPBS, centrifuging at 500 RCF for 5 min and removing the supernatant each time. After the last wash, the resin was resuspended in 625 μl DPBS. To each Ultrafree-MC-HV Durapore PVDF 0.45 μm centrifugal filters (Millipore), 50 μl resin slurry

and cleared lysates were added. Samples were mutated overnight at 4°C. The following day the resin was washed three times with 30 min incubations in Buffer III + G [50 mM HEPES, pH 7.4, 150 mM NaCl, 0.02% Cholesteryl hemisuccinate (CHS)], 0.1% DDM, 0.1% 3-[(3-cholamidopropyl)-dimethylammonio]-1-propane sulfonate] (CHAPS), and 50 nM 1,2-dioleoyl-sn-glycero-3-phosphocholine (DOPC)/1,2-dioleoyl-sn-glycero-3-phospho-L-serine (DOPS) (7:3), 10% glycerol), before the purified receptor was eluted in 30 μl elution buffer [Buffer III + G, 0.33 mg/mL 1D5 peptide (TETSQVAPA). A total of 19.5 μl of the elution was incubated with NuPAGE™ LDS Sample Buffer (Invitrogen) and 100 mM DTT prior to gel electrophoresis in 1.5 mm × 15 well NuPAGE™ 4%–12% Bis-Tris (Invitrogen) gels run in NuPAGE™ MES-SDS Running Buffer (Invitrogen) at a constant voltage of ~115 V. The gel was then transferred onto Immobilon PVDF-FL membrane (Millipore), then incubated in Intercept Blocking Buffer (IBB, LI-COR Biosciences) for 1 h, RT. Primary antibody solution [IBB + 0.1% Tween 20 + 1:2000 dilution anti-1D4 mouse mAb (MacKenzie et al., 1984) ± 1:2000 anti-OLLAS rat (Park et al., 2008)] was incubated at RT for 1 h. Membranes were washed five times in wash buffer (DPBS + 0.1% Tween-20) for 4 min prior to 1 h incubation in secondary antibody solution (IBB + 0.1% Tween 20 + 0.01% SDS, +1:10,000 IRDye 800CW goat anti-mouse IgG (LI-COR Biosciences, 926-32210) or +1:10,000 IRDye 680RD goat anti-mouse antibody (Invitrogen, A32729) and 1:10,000 IRDye 800CW goat anti-rat antibody (Rockland Immunochemicals, 612-131-120). Membranes were washed five times in wash buffer then twice in DPBS prior to imaging using a LI-COR Odyssey M infrared laser scanning imager.

CONFLICT OF INTEREST
The authors declare no competing financial interests.

DATA AVAILABILITY STATEMENT
The data that supports the findings of this study are available in the supplementary material of this article. Additional data or plasmids available upon request.

ORCID
Jordan M. Mattheisen https://orcid.org/0000-0002-9334-9521
Jaina S. Wollowitz https://orcid.org/0000-0002-5938-4382
Thomas P. Sakmar https://orcid.org/0000-0002-2836-8953

REFERENCES
Agard NJ, Prescher JA, Bertozzi CR. A strain-promoted [3 + 2] azide-alkyne cycloaddition for covalent modification of biomolecules in living systems. J Am Chem Soc. 2004;126(46):15046–7.

Berchiche YA, Sakmar TP. CXC chemokine receptor 3 alternative splice variants selectively activate different signaling pathways. Mol Pharmacol. 2016;90(4):483–95.

Blackman ML, Royzen M, Fox JM. Tetrazine ligation: fast bioconjugation based on inverse-electron-demand Diels-Alder reactivity. J Am Chem Soc. 2008;130(41):13518–9.

Chin JW, Cropp TA, Anderson JC, Mukherji M, Zhang Z, Schultz PG. An expanded eukaryotic genetic code. Science. 2003;301(5635):964–7.

Chin JW, Cropp TA, Chu S, Meggers E, Schultz PG. Progress toward an expanded eukaryotic genetic code. Chem Biol. 2003;10(6):511–9.

Conklin BR, Farfel Z, Lustig KD, Julius D, Bourne HR. Substitution of three amino acids switches receptor specificity of Gq alpha to that of Gi alpha. Nature. 1993;363(6426):274–6.

Dommerholt J, Rutjes F, van Delft FL. Strain-promoted 1,3-dipolar cycloaddition of cycloalkynes and organic azides. Top Curr Chem (Cham). 2016;374(2):16.

Dommerholt J, Schmidt S, Temming R, Hendriks LJ, Rutjes FP, van Hest JC, et al. Readily accessible bicyclononynes for bioorthogonal labeling and three-dimensional imaging of living cells. Angew Chem Int Ed Engl. 2010;49(49):9422–5.

Fan F, Wood KV. Bioluminescent assays for high-throughput screening. Assay Drug Dev Technol. 2007;5(1):127–36.

Gagnon L, Cao Y, Cho A, Sedki D, Huber T, Sakmar TP, et al. Genetic code expansion and photocross-linking identify different beta-arrestin binding modes to the angiotensin II type 1 receptor. J Biol Chem. 2019;294(46):17409–20.

Grunbeck A, Huber T, Abrol R, Trzaskowski B, Goddard WA 3rd, Sakmar TP. Genetically encoded photo-cross-linkers map the binding site of an allosteric drug on a G protein-coupled receptor. ACS Chem Biol. 2012;7(6):967–72.

Hall MP, Unch J, Binkowski BF, Valley MP, Butler BL, Wood MG, et al. Engineered luciferase reporter from a deep sea shrimp utilizing a novel imidazopyrazinone substrate. ACS Chem Biol. 2012;7(11):1848–57.

Huang LY, Umanah G, Hauser M, Son C, Arshava B, Naider F, et al. Unnatural amino acid replacement in a yeast G protein-coupled receptor in its native environment. Biochemistry. 2008;47(20):5638–48.

Huber T, Sakmar TP. Chemical biology methods for investigating G protein-coupled receptor signaling. Chem Biol. 2014;21(9):1224–37.

Knepp AM, Grunbeck A, Banerjee S, Sakmar TP, Huber T. Direct measurement of thermal stability of expressed CCR5 and stabilization by small molecule ligands. Biochemistry. 2011;50(4):502–11.

Kohrer C, Yoo JH, Bennett M, Schaack J, RajBhandary UL. A possible approach to site-specific insertion of two different unnatural amino acids into proteins in mammalian cells via nonsense suppression. Chem Biol. 2003;10(11):1095–102.

Koole C, Reynolds CA, Mobarec JC, Hick C, Sexton PM, Sakmar TP. Genetically encoded photocross-linkers determine the biological binding site of exendin-4 peptide in the N-terminal domain of the intact human glucagon-like peptide-1 receptor (GLP-1R). J Biol Chem. 2017;292(17):7131–44.

Kowalski-Jahn M, Schihada H, Turku A, Huber T, Sakmar TP, Schulte G. Frizzled BRET sensors based on bioorthogonal labeling of unnatural amino acids reveal WNT-induced dynamics of the cysteine-rich domain. Sci Adv. 2021;7(46):eabj7917.

Lang K, Davis L, Wallace S, Mahesh M, Cox DJ, Blackman ML, et al. Genetic encoding of bicyclononynes and trans-cyclooctenes for site-specific protein labeling in vitro and in live mammalian cells via rapid fluorogenic Diels-Alder reactions. J Am Chem Soc. 2012;134(25):10317–20.

Lorenzen E, Ceraudo E, Berchiche YA, Rico CA, Furstenberg A, Sakmar TP, et al. G protein subtype-specific signaling bias in a series of CCR5 chemokine analogs. Sci Signal. 2018;11(552).

MacKenzie D, Arendt A, Hargrave P, McDowell JH, Molday RS. Localization of binding sites for carboxyl terminal specific anti-rhodopsin monoclonal antibodies using synthetic peptides. Biochemistry. 1984;23(26):6544–9.

Naganathan S, Ye S, Sakmar TP, Huber T. Site-specific epitope tagging of G protein-coupled receptors by bioorthogonal modification of a genetically encoded unnatural amino acid. Biochemistry. 2013;52(6):1028–36.

Oprian DD, Asenjo AB, Lee N, Pelletier SL. Design, chemical synthesis, and expression of genes for the three human color vision pigments. Biochemistry. 1991;30(48):11367–72.

Park SH, Cheong C, Idoyaga J, Kim JY, Choi JH, Do Y, et al. Generation and application of new rat monoclonal antibodies against synthetic FLAG and OLLAS tags for improved immunodetection. J Immunol Methods. 2008;331(1–2):27–38.

Rannversson H, Andersen J, Sorensen L, Bang-Andersen B, Park M, Huber T, et al. Genetically encoded photocrosslinkers locate the high-affinity binding site of antidepressant drugs in the human serotonin transporter. Nat Commun. 2016;7:11261.

Schmied WH, Elsasser SJ, Uttamapinant C, Chin JW. Efficient multisite unnatural amino acid incorporation in mammalian cells via optimized pyrrolysyl tRNA synthetase/tRNA expression and engineered eRF1. J Am Chem Soc. 2014;136(44):15577–83.

Serfling R, Lorenz C, Etzel M, Schicht G, Bottke T, Morl M, et al. Designer tRNAs for efficient incorporation of non-canonical amino acids by the pyrrolysine system in mammalian cells. Nucleic Acids Res. 2018;46(1):1–10.

Serfling R, Seidel L, Bock A, Lohse MJ, Annibale P, Coin I. Quantitative single-residue bioorthogonal labeling of G protein-coupled receptors in live cells. ACS Chem Biol. 2019;14(6):1141–9.

Shah UH, Toneatti R, Gaitonde SA, Shin JM, Gonzalez-Maeso J. Site-specific incorporation of genetically encoded photo-crosslinkers locates the heteromeric interface of a GPCR complex in living cells. Cell Chem Biol. 2020;27(10):1308–1317.e1304.

Tian H, Furstenberg A, Huber T. Labeling and single-molecule methods to monitor G protein-coupled receptor dynamics. Chem Rev. 2017;117(1):186–245.

Tian H, Gunnison KM, Kazmi MA, Sakmar TP, Huber T. FRET sensors reveal the retinal entry pathway in the G protein-coupled receptor rhodopsin. iScience. 2022;25(4):104060.

Tsien RY. The green fluorescent protein. Annu Rev Biochem. 1998;67:509–44.

van Geel R, Pruijn GJ, van Delft FL, Boelens WC. Preventing thiol-yne addition improves the specificity of strain-promoted azide-alkyne cycloaddition. Bioconjug Chem. 2012;23(3):392–8.

Wang L, Brock A, Herberich B, Schultz PG. Expanding the genetic code of Escherichia coli. Science. 2001;292(5516):498–500.

Wang L, Magliery TJ, Liu DR, Schultz PG. A new functional suppressor tRNA/aminoacyl−tRNA synthetase pair for the in vivo incorporation of unnatural amino acids into proteins. J Am Chem Soc. 2000;122(20):5010–1.

Wang L, Schultz PG. A general approach for the generation of orthogonal tRNAs. Chem Biol. 2001;8(9):883–90.

Wang X, Liu D, Shen L, Li F, Li Y, Yang L, et al. A genetically encoded F-19 NMR probe reveals the allosteric modulation mechanism of cannabinoid receptor 1. J Am Chem Soc. 2021;143(40):16320–5.

Wangen JR, Green R. Stop codon context influences genome-wide stimulation of termination codon readthrough by aminoglycosides. Elife. 2020;9.

Ye S, Huber T, Vogel R, Sakmar TP. FTIR analysis of GPCR activation using azido probes. Nat Chem Biol. 2009;5(6):397–9.

Ye S, Kohrer C, Huber T, Kazmi M, Sachdev P, Yan ECY, et al. Site-specific incorporation of keto amino acids into functional G protein-coupled receptors using unnatural amino acid mutagenesis. J Biol Chem. 2008;283(3):1525–33.

Ye S, Zaitseva E, Caltabiano G, Schertler GF, Sakmar TP, Deupi X, et al. Tracking G-protein-coupled receptor activation using genetically encoded infrared probes. Nature. 2010;464(7293):1386–9.

Zhou W, Wesalo JS, Liu J, Deiters A. Genetic code expansion in mammalian cells: a plasmid system comparison. Bioorg Med Chem. 2020;28(24):115772.

SUPPORTING INFORMATION

Additional supporting information can be found online in the Supporting Information section at the end of this article.